First analysis of the NAWDEX field campaign

Meryl WIMMER
M2 SOAC - DC

1 Introduction

Extratropical cyclones are meteorological phenomena associated with low pressure that play an essential role in the general atmospheric circulation of mid-latitudes. However, despite constant improvements in numerical weather prediction models[1], there is still room for improvement in the quality of these forecasts, particularly for extreme events. One source of error concerns the representation of diabatic processes (cloud microphysics, radiation, turbulence), particularly in the Warm Conveyor Belt (WCB), a mass of warm moist air that rises in cyclones.

To better understand the impact of these diabatic processes and improve their representation in numerical models, the Predictability and Dynamical Processes group of the THORPEX [a] program proposed the international NAWDEX [b] project in 2014.

This project, supported by the World Weather Research Programme of the World Meteorological Organisation, mainly brings together American and Europe and countries such as Germany, the United Kingdom, the United States, France and Canada. In autumn 2016, thanks to the deployment of 4 research aircraft and ground instrumentation in Iceland and Western Europe, it was possible to set up a measurement campaign to sample WCBs.

Here, a first analysis of the NAWDEX campaign is carried out, more specifically, on the case of the extratropical cyclone of 02nd of October 2016. So far, only flight F7 of the Falcon 20 of the Safire team (Service des avions français instrumentés pour la recherche en environnement), which measured the rising part of a WCB, has been studied. A series of 24-hour Lagrangian trajectories, initialised along the aircraft's path, were calculated from the outputs of the ARPEGE model (Action de Recherche Petite Echelle Grande Echelle)[2].

In this report, we will first review the state of the art of WCBs. Then, we will present the method used during this internship to calculate Lagrangian trajectories. In section 4, we will briefly analyse the results obtained. Finally, we will conclude.

2 Warm Conveyor Belt

Within extratropical cyclones, three air masses or conveyor belts are identified: the dry intrusion, the cold conveyor belt and the warm conveyor belt (WCB)[3]. The latter corresponds to a mass of warm moist air originating in the subtropical marine atmospheric boundary layer and rising to near 280hPa in the upper troposphere, towards the poles. These WCBs are therefore identified by a decrease of 600hPa in 48 hours[4]. They occur mainly in winter, over the oceans, particularly over the North Atlantic and the North Pacific ocean[5].

As the moist air rises, it condenses, forming clouds. These WCBs are therefore particularly recognisable on satellite images, as they are the main cloud band of extratropical cyclones. Since clouds are the site of diabatic processes such as the production of latent heat by condensation, the potential temperature can rise by 20 to 40 K. However, other thermodynamic quantities are modified by the presence of a WCB.

Potential vorticity (PV) is a conservative quantity in adiabatic and frictionless atmosphere, whose temporal tendency:

$$\frac{dq}{dt} = -\frac{1}{\rho}\left[(f+\xi)\nabla\dot{\theta} + \nabla \wedge F.\nabla\theta\right] \quad (1)$$

where q is the potential vorticity, ρ the air density, f the Coriolis parameter, ξ the relative vorticity, θ the potential temperature and F the friction force. According to equation 1, PV can be produced or destroyed by a heating gradient $\nabla\dot{\theta}$ resulting from the emission of sensible or latent heat, or from radiation or turbulence (first term of equation 1). It can also be modified by the effect of turbulence on the wind (second term of equation 1).

[a] The Observing System Research and Predictability Experiment

[b] North Atlantic Waveguide Downstream Impact EXperiment: http://nawdex.ethz.ch/

Thus, when there is a heating maximum, PV is produced below this maximum and destroyed above it. In addition, Chagnon[6] has shown, by separating the different sources of heating, that the production of PV below the heating maximum was due mainly to boundary layer phenomena (convection and turbulence) and the destruction of PV above, to radiation.

Once it reaches the tropopause, the WCB can take two different directions: either it wraps around the low-pressure core and forms the cloud head of the extratropical cyclones, or it is caught up in the upper anticyclonic flows located downstream of the jet stream.

3 Lagrangian trajectories and method validation

3.1 Lagrangian trajectory algorithm

Given a 3D wind field, a trajectory model can reconstruct the trajectory of an air particle from a seeding point. The position of an air particle $x(t)$ can be obtained by numerically integrating, between two instants, $dx/dt = \mathbf{v}(x)$. To do this, we need to know the value of the wind at the mid-point between these two instants. However, as the final position is undetermined, so this mid-point is also undetermined. It is therefore necessary to use iterative methods (predictor-corrector scheme) to build the solution step by step.

There are various models of Lagrangian trajectories, but the LAGRANTO software package, developed by ETH [c], is particularly well suited to producing trajectories with WCB characteristics[7].

By analogy with the LAGRANTO software, we have, from a code developed by students at the Ecole National de la Météorologie, produced a set of 12-hour backward and forward trajectories, seeded along the aircraft's path. The aim here is to study the diabatic processes undergone by air particles before and after the flight.

We therefore used the data of the ARPEGE forecast starting the 1rst of October 2016 at 12UTC, namely one day before the flight F7.

[c]Eidgenössische Technische Hochschule Zürich

Since the potential temperature and wind tendencies used to calculate PV tendency are provided on an irregular grid that differs from that of the standard meteorological data, different methods were used to obtain the values of these variables at the trajectory points.

The method used here performs a first interpolation so that all the variables are on the same regular grid, then performs a second interpolation to obtain these variables at the trajectory position. In addition, we have data from two different versions of ARPEGE (analysed below): the version operational in 2016, referred to here as Run0, and a version including the PCMT [d 8] convection scheme, referred to as Run6.

3.2 IOP 6 : 1-5 October 2016

During this internship, we studied the extratropical cyclones occuring of 02nd od October 2016 in the Atlantic Ocean. It formed off Newfoundland on 01st of October and intensified as it moved eastwards. It reached its peak on 02nd of October with a minimum of mean sea level surface pressure of 960hPa at 21hUTC off Iceland. The surface anomaly coincide with a very low of geopotential in mid-troposphere (figure 1). The meteorological situation is somewhat unusual: a ridge of high pressure stretches from Spain to Ireland, forming a high-pressure system over Scandinavia on 3rd of October. This high-pressure system will persist over Europe, creating a blocking situation for around ten days.

Scientific flights were carried out off Iceland on 2nd October. The SAFIRE Falcon 20, with a LNG lidar, a 95GHz RASTA doppler radar (RALI) and an infrared radiometer on board, took off from Keflavik at 13:00 UTC for a flight lasting 3 hours and 15 minutes. The aircraft's trajectory can be seen in figure 1.

At the time of the flight, the pressure minimum of the cyclone was to the south-west of Iceland. The aircraft remained to the east of this minimum in order to be in the WCB part of the cyclone, as we shall see later.

[d]Prognostic Condensates Microphysics and Transport

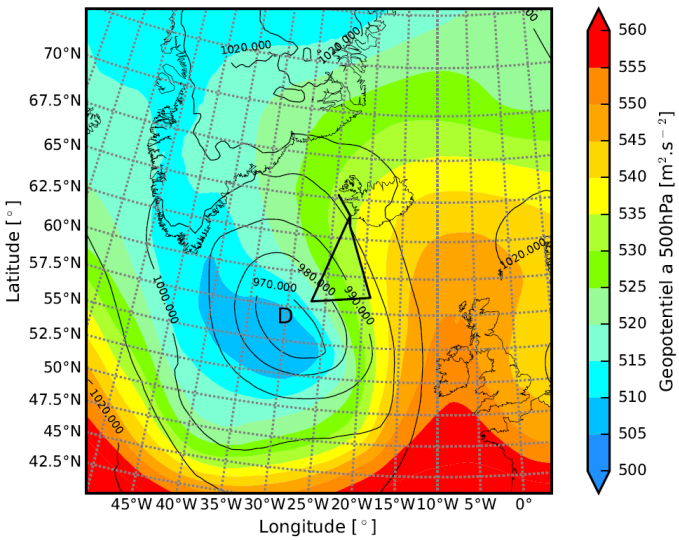

Figure 1: *ARPEGE analysis map of geopotential at 500hPa (shading) and pressure (in hPa) at mean sea level (isoline) at 12UTC on 02nd of October 2016. The path of flight F7 is shown as a black line to the south-west of Iceland*

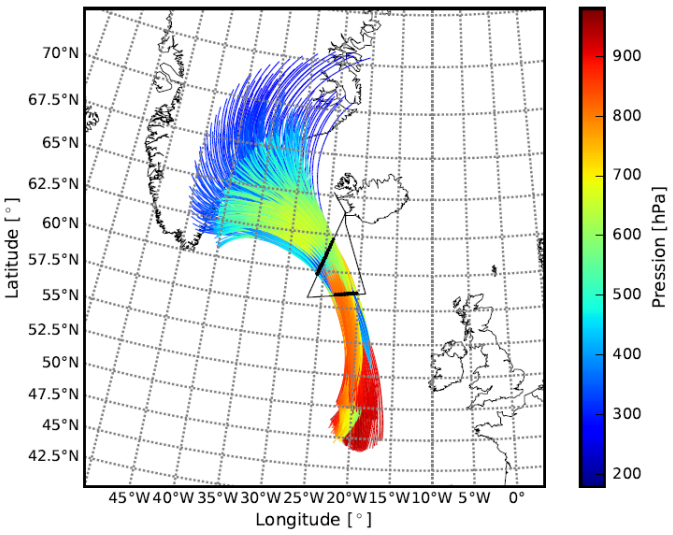

Figure 2: *Pressure along the 24-hour trajectories for Run0. The black dots are the seeding points along the flight (black solid line)*

3.3 Lagrangian trajectories seeding

The trajectories were seeded at 84 grid points along the aircraft's path and at 63 different levels, ranging from 975hPa to 187.5hPa. This gives us almost 5,000 trajectory seeding points. Since the flight has a triangle shape, these seedings were split according to each side of the triangle. We then combined the forward and backward trajectories to obtain 24-hour trajectories centred on the time of flight. In order to keep only those with WCB properties, we applied the 300hPa criterion over 24 hours. As no 48-hour trajectories were available, the Joos and Wernli criterion of 600hPa in 48 hours was simply halved[4].

For greater precision, and as proposed by Sprenger and Wernli[7], we added a second criterion on temperature : an increase of 15°C in 12 hours. This criterion is slightly more restrictive than the one recommended by Sprenger and Wernli (10°C in 48h)[7]. Thus, by applying these two criteria, we obtain 485 trajectories identified as WCB for Run 0 and 501 for Run 6 (figure 2).

3.4 Validation of forecasts using campaign observations

As the aircraft was equipped with Doppler radar, it was possible to measure the wind along the aircraft's path. Figure 3 shows that the mean vertical wind profiles in the WCB for the two versions of ARPEGE give similar results and are consistent with the observations: these profiles are within 68% of the observed values. However, the wind minimum at 700hPa, in the WCB trajectories zone, is not perfectly represented: it is overestimated in Run6 and underestimated for Run0. As we cannot say whether one of these two forecasts is better than the other, we have decided to keep both in order to get an uncertainty view in our interpretations.

4 Analysis of diabatic processes along WCB trajectories

Figure 2 shows that there are several distinct types of WCB trajectories. Some trajectories appear to have a cyclonic curvature over the last two hours, while others have an anticyclonic curvature. We therefore separated these trajectories by calculating the average curvature over the last two hours. Over 75% (83% for Run0 and 78% for Run6) of the WCB par-

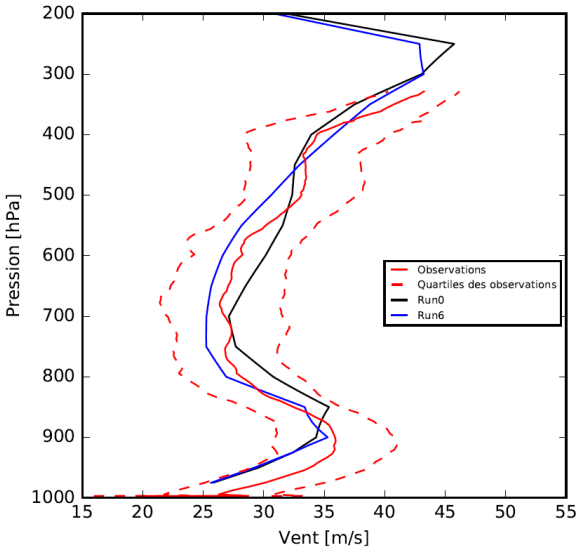

Figure 3: *Averaged vertical profiles of horizontal wind in the WCB. In red, in-situ measurements. In black, Run0. In blue, Run6. Difference between the solid red line and the dashed line: standard deviation of the observations.*

ticles were in the upper-level anticyclonic flow. We therefore focused our attention on these particles.

On figure 4, we notice that almost all anticyclonic particles (coloured dots) reach, at the end of their path around 300hPa, a zone of low PV. This is the anticyclone settling over Europe. These particles bring low PV, due to diabatic processes, to the ridge. Indeed, this bringing of negative PV, reducing the PV aloft in the anticyclonic zone, can explain the strengthening of the PV gradient and the intensification of the anticyclone leading to a blocking situation during the following days.

Figure 5 confirms a loss of PV ($\Delta PV < 0$) for most of the particles (boxplot n°1). This conclusion can also be done from the sum of the temporaly integrated PV tendency (PV due to the effects of turbulence on wind and the effects of sensible and latent heat, radiation and turbulence on temperature)(boxplot n°7). These two boxplots have very similar averages (red square), around -0.25 PVU, which confirms the robustness of our results for both versions of ARPEGE. However, the distribution of these boxplots is different, particularly for Run6 where the distribution reaches very negative PV values. One of the reasons for these differences may lie in the fact that horizontal diffusion is not taken into account.

This drop in PV, although occurring in both runs, does not have the same origins. For Run0, the negative part comes mainly from the effects of turbulence on the wind (boxplot n°3). For Run6, on the other hand, it is mainly due to heating (boxplot no. 2). More specifically, the diabiatic origin seems to be the heating due to sensible and latent heat (boxplot 4). Note that for Run0, this terms is positive. Wet processes therefore do not have the same influence on PV for the two runs. Their predominance is not established, contrary to what we expected.

The origin of the negative PV is equally plausible for both runs, so for the moment it is impossible to determine which of the two runs is the more realistic. Furthermore, for both versions of ARPEGE, radiation seems to have little impact on altitude dynamics, which contradicts the work carried out by Chagnon[6].

5 Conclusion

Using a set of trajectories seeded along a flight made in October 2016 off Iceland, a study of the impact of diabatic processes within the WCBs was carried out. The contribution of negative PV near tropopause helped to intensify the anticyclone setting up over Scandinavia and creating a blocking situation over the following days. Although the two analyzed forecast show a destruction of PV in high troposphere, the diabatic processes at the origin are different. In order to continue our study of the impact of diabatic processes downstream of the jet stream, we are going to study the data from a flight occuring during the morning of 02nd of October, which sampled the outflow from the WCB. Using data from dropsondes launched during this flight, we can hope to determine which of the two runs is more realistic.

Furthermore, we have only used wind data to validate our two runs. Other variables could be studied: relative humidity, temperature, but also ice water content data, that can be estimated from RASTA radar, LNG lidar and infrared radiometer data[9].

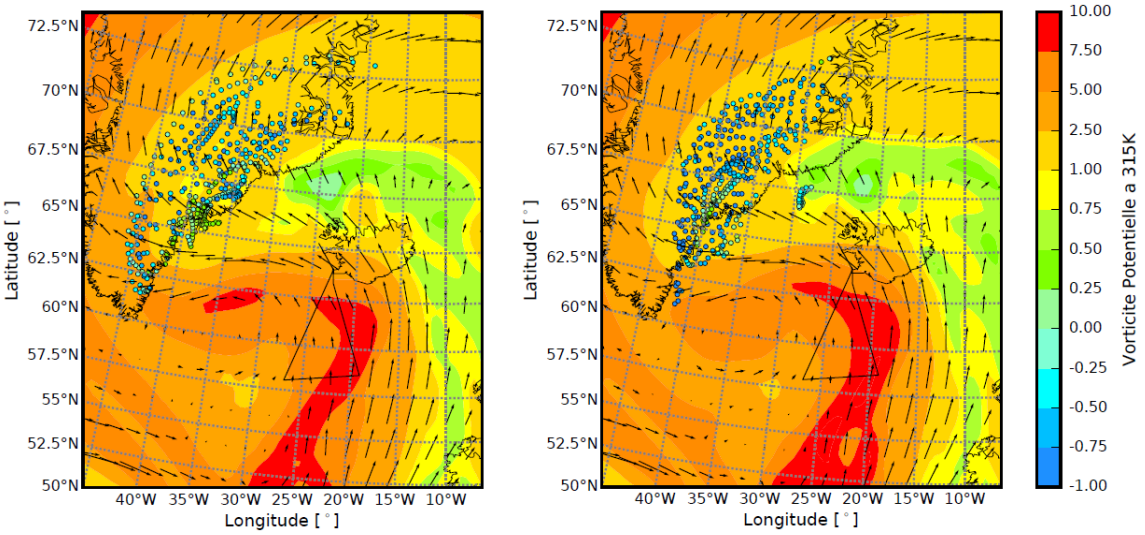

Figure 4: *Map of PV and horizontal wind at 315K for Run0 (left) and Run6 (right) with coloured dots showing the difference in PV between the start and end of the trajectories at their final location.*

References

[1] P. Bauer, A. Thorpe, and Brunet G. The quiet revolution of numerical weather prediction. *Nature*, 525, septembre 2015.

[2] S. Dirren, M. Didone, and H.C. Davies. Diagnoses of "forecast-analysis" differences of a weather prediction system. *Geophysical Research Letters*, 30 (20), 2003.

[3] T.N. Carlson. Airflow through midlatitude cyclones and the comma cloud pattern. *Monthly Weather Review*, 108, 1980.

[4] H. Joos and H. Wernli. Influence of microphysical processes on the potential vorticity development in a warm conveyor belt: a case-study with the limited-area model cosmo. *Quaterly Journal of the Royal Meteorological Society*, 138, January 2012.

[5] E. Madonna et al. Warm conveyor belt in the era-interim dataset (1979-2010). part i: Climatology and potential vorticity evolution. *Journal of Climate*, 27, January 2014.

[6] J.M. Chagnon, S. L. Gray, and J. Methven. Diabatic processes modifying potential vorticity in a north atlantic cyclone. *Quaterly Journal of the Royal Meteorological Society*, 139, July 2013.

[7] M. Sprenger and H. Wernli. The lagranto lagrangian analysis tool - version 2.0. *Geoscientific Model Development*, 8, 2015.

[8] J.-M. Piriou et al. An approach for convective parametrization with memory: Separating microphysics and transport in grid-scale equations. *Journal of the Atmospheric Sciences*, 64, 2007.

[9] J. Delanoe and J. Hogan. A variational scheme for retrieving ice cloud properties from combined radar, lidar and infrared radiometer. *Journal of Geophysical Research*, 113, 2008.

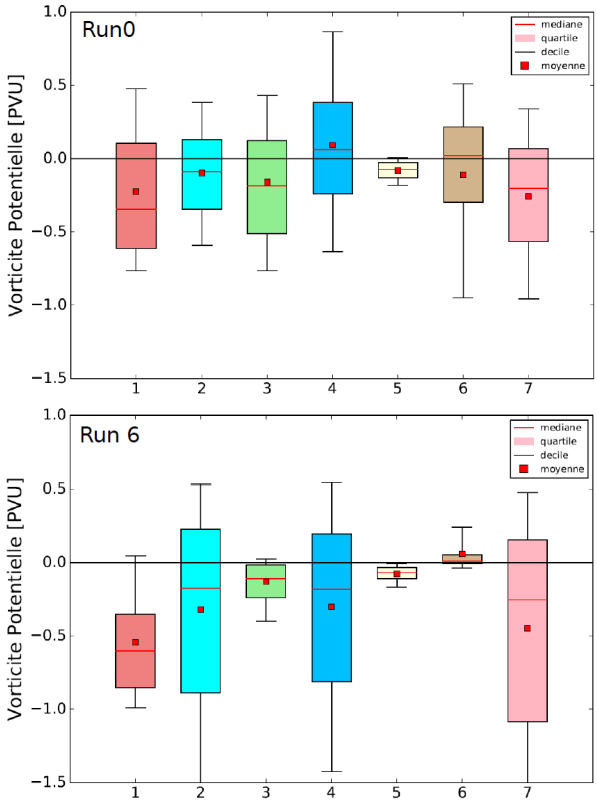

Figure 5: *Distribution of diabatic PV at the end of anticyclonic trajectories. 1: difference in PV between the beginning and the end of the trajectories; 2: PV due to heating (sum of boxplots 4, 5 and 6); 3: PV due to the effects of turbulence on the wind; 4: PV due to sensible and latent heat; 5: PV due to radiation; 6: PV due to the effects of turbulence on temperature; 7: sum of boxplots 2 and 3.*